0026-895X/03/6401-11–20$7.00
MOLECULAR PHARMACOLOGY
Copyright © 2003 The American Society for Pharmacology and Experimental Therapeutics
Mol Pharmacol 64:11–20, 2003

Vol. 64, No. 1
2047/1071077
Printed in U.S.A.

Spatial Regulation of Gαi Protein Signaling in Clathrin-Coated Membrane Microdomains Containing GAIP

ERIC ELENKO, THIERRY FISCHER, INGRID NIESMAN, TIM HARDING, TAMMIE MCQUISTAN, MARK VON ZASTROW, and MARILYN G. FARQUHAR

Departments of Cellular and Molecular Medicine (E.E., T.F., I.N., T.H., T.M., M.G.F.) and Pathology (T.H., M.G.F.), University of California San Diego, La Jolla, California; and Department of Psychiatry (M.V.Z.), University of California San Francisco, San Francisco, California

Received August 2, 2002; accepted March 21, 2003

This article is available online at http://molpharm.aspetjournals.org

ABSTRACT

Regulators of G-protein signaling (RGS) proteins are GTPase-activating proteins (GAPs) that bind to Gα subunits and attenuate G protein signaling, but where these events occur in the cell is not yet established. Here we investigated, by immunofluorescence labeling and deconvolution analysis, the site at which endogenous Gα-interacting protein (GAIP) (RGS19) binds to Gαi3-YFP and its fate after activation of δ-opioid receptor (DOR). In the absence of agonist, GAIP is spatially segregated from Gαi3 and DOR in clathrin-coated domains (CCPs) of the cell membrane (PM), whereas Gαi3-YPF and DOR are located in non–clathrin-coated microdomains of the PM. Upon addition of agonist, Gαi3 partially colocalizes with GAIP in CCPs at the PM. When endocytosis is blocked by expression of a dynamin mutant [dyn(K44A)], there is a striking overlap in the distribution of DOR and Gαi3-YFP with GAIP in CCPs. Moreover, Gαi3-YFP and GAIP form a coprecipitable complex. Our results support a model whereby, after agonist addition, DOR and Gαi3 move together into CCPs where Gαi3 and GAIP meet and turn off G protein signaling. Subsequently, Gαi3 returns to non–clathrin-coated microdomains of the PM, GAIP remains stably associated with CCPs, and DOR is internalized via clathrin-coated vesicles. This constitutes a novel mechanism for regulation of Gα signaling through spatial segregation of a GAP in clathrin-coated pits.

Ligand binding to G protein-coupled receptors (GPCRs) causes activation of Gα and Gβγ subunits that in turn regulate multiple downstream effectors. Signaling is shut off by regulators of G protein signaling (RGS) proteins that bind Gα subunits through a conserved RGS domain and act as GTPase-activating proteins (GAPs), accelerating GTP hydrolysis and inactivation (De Vries et al., 2000; Ross and Wilkie, 2000). The orchestration of these events and their localization at the cellular level is a topic of high current interest. Many GPCRs are thought to be associated in part with lipid rafts or caveolae (Shaul and Anderson, 1998) on the plasma membrane (PM). After ligand binding, they cluster in clathrin-coated pits, undergo dynamin-mediated endocytosis via clathrin coated vesicles (CCVs) (Ferguson, 2001), and traffic to early endosomes, where they are sorted for recycling to the PM or delivered to lysosomes and degraded (Tsao and von Zastrow, 2001). Gαi subunits are assumed to interact with GPCR at the PM (Neubig, 1994; Wedegaertner et al., 1996; Huang et al., 1997; Fishburn et al., 2000) and to remain at the PM after receptor internalization (Wedegaertner, 1998; Hughes et al., 2001). Nothing is known, however, about where interaction between RGS proteins and Gα proteins occurs or the fate of the GAP after this interaction.

We previously showed that GAIP (RGS19), which acts as a GAP for the Gαi subfamily of G proteins (De Vries et al., 1995), is localized on clathrin-coated pits or microdomains (CCPs) on both the PM and the trans-Golgi network (De Vries et al., 1998). The localization of an RGS protein on CCPs raises questions about where GAIP interacts with Gαi and its fate after receptor internalization.

To investigate these questions, we used a cell line, 293SFDOR, that stably expresses FLAG-tagged, δ-opioid receptor (DOR), a Gαi-linked GPCR, because the trafficking of this receptor has been well characterized in these cells (Tsao and von Zastrow, 2001; Whistler et al., 2001). DOR is known to be phosphorylated upon agonist binding (Whistler et al., 2001), internalized in clathrin-coated vesicles (Keith et al., 1996), and subsequently targeted to lysosomes where it is degraded (Tsao and von Zastrow, 2000).

This work was supported by National Institutes of Health grants CA58689 and DK17780 (to M.G.F) and training grants CA67754 and HL0726 (to E.E.).

ABBREVIATIONS: GPCR, G protein-coupled receptor; GAP, GTPase-activating protein; RGS, Regulators of G-protein signaling; PM, plasma membrane; CCV, clathrin-coated vesicle; GAIP, Gα-interacting protein; CCP, clathrin-coated domain of the cell membrane; DOR, δ-opioid receptor; DPDPE, [D-Pen^2,D-Pen^5]-enkephalin; mAb, monoclonal antibody; GFP, green fluorescent protein; YFP, yellow fluorescent protein; HRP, horseradish peroxidase; HA, hemagglutinin; PAGE, polyacrylamide gel electrophoresis; PBS, polyacrylamide gel electrophoresis; PFA, paraformaldehyde; EM, electron microscopy ; PNS, postnuclear supernatant; AP-2, activator protein 2; EEA1, early endosome antigen 1.

Our results support a dynamic model for the spatial regulation of G protein signaling whereby activated, GTP-bound Gαi subunits together with activated DOR move from noncoated to clathrin-coated microdomains of the PM, where they bind GAIP. The inactivated (GDP-bound) Gαi subunits presumably move back to noncoated microdomains of the PM, DOR are internalized, and GAIP remains stably associated with CCPs.

Materials and Methods

Animals and Reagents. [D-Pen^2,D-Pen^5]-enkephalin (DPDPE) and protease inhibitor cocktail were purchased from Sigma (St. Louis, MO), the chemiluminescence detection kit from Pierce (Rockford, IL), and Alexa Fluor-568 conjugated human transferrin from Molecular Probes (Eugene, Oregon).

Antibodies. Anti-GAIP (N) and anti-GAIP (C) raised against the N and C termini, respectively, of GAIP were characterized previously (De Vries et al., 1998). Mouse monoclonal (mAb) AP-2 α-adaptin and dynamin-1 were provided by Dr. Sandra Schmid (The Scripps Research Institute, La Jolla, CA). Anti-GFP serum (which recognizes both GFP and YFP) was a gift from Dr. Charles Zuker (University of California San Diego, La Jolla, CA), and the anti-GFP mAb (JL-8, IgG_{2a}) was from BD Biosciences Clontech (Palo Alto, CA). Affinity-purified rabbit IgG against the common C terminus of Gβ subunits (T20) was from Santa Cruz Biotechnology (Santa Cruz, CA), anti-FLAG (M2) was from Sigma-Aldrich, and polyclonal anti-clathrin heavy chain was from Affinity BioReagents (Golden, CO). The anti-HA and anti-early endosome antigen 1 (EEA1) mAbs were from Covance Research Products (Richmond, CA) and BD Transduction Laboratories (Lexington, KY), respectively. HRP-conjugated goat anti-rabbit IgG was from Bio-Rad (Hercules, CA). Highly cross-absorbed Alexa Fluor-488 goat anti-rabbit and Alexa Fluor-594 goat anti-mouse $F(ab')_2$ were from Molecular Probes (Eugene, OR), and goat anti-rabbit and anti-mouse IgG gold (5 or 10 nm) conjugates were from Amersham Biosciences (Piscataway, NJ).

Cell Culture, Transfection, and Ligand Uptake. Human embryonic kidney 293 cells (293SFDOR) that stably express FLAG-tagged DOR (Keith et al., 1996) were used for all the experiments. They were grown in Dulbecco's modified Eagle's/high glucose media supplemented with 10% (v/v) fetal bovine serum, 100 U/ml penicillin G, 100 U/ml streptomycin sulfate, and 0.3 mg/ml glutamine (Invitrogen, Carlsbad, CA). In some cases, these cells were transfected with cDNA encoding HA-tagged, dominant-negative dyn(K44A) in the pCB vector (obtained from Dr. Sandra Schmid) and/or cDNA encoding for Gαi3-YFP in the pcDNA3 vector (Weiss et al., 2001) using FuGENE6 (Roche Applied Science, Palo Alto, CA); 24 h after transfection, they were processed for immunofluorescence and immunoelectron microscopy. In some cases, culture medium was replaced with Dulbecco's modified Eagle's/high-glucose media containing either 5 μM DPDPE or 5 mg/ml Alexa Fluor-568 transferrin (Molecular Probes; Eugene, OR), for 1 to 30 min before processing for immunocytochemistry or immunoprecipitation analysis.

Subcellular Fractionation, SDS-PAGE, and Immunoblotting. Cells were scraped into ice-cold PBS containing protease inhibitors, passed (10 times) through a 30.5-gauge needle and centrifuged at 600*g* for 5 min at 4°C. The resulting postnuclear supernatant was centrifuged (100,000*g*), and the pellet (crude membrane fraction) was resuspended in a volume of PBS equal to that of the supernatant. Proteins present in the supernatant and pellet were separated on 12% SDS-polyacrylamide gels, transferred to polyvinylidinedifluoride membranes (Millipore, Bedford, MA) and immunoblotted with anti-GAIP (N) (1:3000) followed by HRP-conjugated goat anti-rabbit IgG (1:3000) in 5% fetal calf serum/PBS, 0.1% Tween 20, for 1 h each. Detection was by enhanced chemiluminescence.

Immunoprecipitation. Cells were transfected with pcDNAGαi3-YFP, pCBHA-dyn(K44A), and GAIP in the pcDNA3 vector (De Vries et al., 1996) as described above. Eighteen hours after transfection, cells were homogenized in TBS containing protease inhibitors supplemented with (1 mM $NaVO_4$ and 1 mM NaF); crude membrane and cytosolic fractions were prepared as described above and solubilized for 30 min in buffer A [0.5% deoxycholate, 1% Nonidet P-40, 50 mM Tris, 150 mM NaCl, 1 mM EDTA, and 2.5 mM $MgCl_2$ (Levis and Bourne, 1992)]. Gαi3-YFP was immunoprecipitated from both cytosolic and membrane fractions using the anti-GFP mAb and collected on protein A Sepharose CL-4B (Amersham Biosciences, Piscataway, NJ). Immune complexes were washed three times in solubilization buffer and separated on 12% SDS-PAGE. Proteins were transferred onto polyvinylidene difluoride membranes and immunoblotted with anti-GAIP (N) or anti-GFP mAb followed by protein A-HRP or goat anti-mouse IgG.

Immunofluorescence and Immunoelectron Microscopy. Cells were fixed in 2% paraformaldehyde (PFA) in 100 mM phosphate buffer, pH 7.4, for 25 min, permeabilized with 0.1% Triton X-100 in PBS (10 min), and incubated for 1 h with primary rabbit polyclonal or mouse mAbs, followed by incubation (1 h) with Alexa Fluor-594 goat anti-mouse and/or Alexa Fluor-488 goat anti-rabbit $F(ab')_2$. For preparation of semithin cryosections, cells were fixed with 4% PFA in the same buffer (45 min) followed by 8% PFA (15 min) at 4°C. Samples were then cryoprotected and frozen in liquid nitrogen (De Vries et al., 1998). Sections (0.5–1.0 μm) were cut at −100°C using a Leica Ultracut UCT microtome with a Leica EMFCS cryoattachment (Leica, Bannockburn, IL) and incubated in primary antibodies (2 h) followed by appropriate secondary antibodies (1 h). Cells and semithin sections were analyzed by deconvolution microscopy with the DeltaVision imaging system (Applied Precision, Issaquah, WA) coupled to a Zeiss S100 fluorescence microscope (Carl Zeiss, Thornwood, NY). For cross-sectional images of cells, stacks were obtained with a 150-nm step-width to optimize reconstruction of the center plane image. Deconvolution was done on an SGI workstation (Mountain View, CA) using Delta Vision reconstruction software, and images were processed as TIF files using Photoshop 5.5 (Adobe Systems, Mountain View, CA).

Fluorescence images of double-labeled samples were quantified as follows: PM areas were traced and selected using Photoshop, and pixel areas with a pixel intensity of 50 or more were measured for red, green and yellow pixels using NIH Image 1.62 software (http://rsb.info.nih.gov/nih-image/) (see Fig. 2). Data were expressed as percentage of overlap with total GAIP or Gαi3-YFP pixels.

For immunogold labeling at the electron microscope (EM) level (De Vries et al., 1998), cells were fixed and cryoprotected as for semithin sections. Ultrathin cryosections were prepared, placed on glow-discharged nickel grids, stored on 2% gelatin/PBS at 4°C, and incubated with primary antibodies followed by 5 or 10 nm gold, goat anti-rabbit, or anti-mouse IgG in 10% fetal calf serum in PBS. Grids were absorption stained with 0.2% neutral uranyl acetate, 0.2% methyl cellulose, and 3.2% polyvinyl alcohol.

For routine EM, cells were fixed with 2.5% glutaraldehyde in 0.1 M cacodylate buffer for 2 h at room temperature, postfixed in 1% OsO_4 in 0.1 M cacodylate buffer (1 h) at room temperature, and embedded as monolayers in LX-112 (Ladd Research, Williston, VT) as described previously (De Vries et al., 1998). Sections were stained in uranyl acetate and lead citrate and observed with the use of an electron microscope (JEOL 1200 EX-II or Philips CM-10).

Results

GAIP Is Entirely Membrane Bound in 293SFDOR Cells. Previously, we reported that GAIP is distributed in both membrane and cytosolic fractions, and the amount found in the two pools varies (60–90%) among different cell types. The membrane pool is largely associated with CCPs

and CCVs and is most probably anchored to membranes via palmitoylation (De Vries et al., 1996). When we determined the distribution of GAIP in membrane (100,000*g* pellet) and cytosolic (100,000*g* supernatant) fractions prepared from 293SFDOR cells, virtually all the GAIP found in the postnuclear supernatant (PNS) pelleted with the membrane fraction (Fig. 1), indicating that GAIP is largely or exclusively associated with membranes in these cells.

GAIP Colocalizes with Clathrin, AP-2, and Dynamin. The distribution of GAIP in 293SFDOR cells resembled that seen in other cell types in that it was found in a punctate pattern along the cell membrane (PM) and in the Golgi region by immunofluorescence (Fig. 2). To verify that GAIP is found in CCPs in these cells, we carried out double immunofluorescence labeling for GAIP and CCV markers [i.e., clathrin, AP-2, and dynamin (Brodsky et al., 2001)], before and immediately after stimulation with the DOR agonist DPDPE, followed by deconvolution analysis. We found that the distribution of GAIP overlaps with all three of these markers. When the percentage of GAIP staining that overlaps with these markers along the PM was quantified as shown in Fig. 2, the overlap of GAIP with clathrin varied from 30 to 50% (Fig. 2), AP-2 from 25 to 40% (Fig. 3, A and B), and dynamin from 10 to 25% (Fig. 3C). There was also a trend toward increased overlap after agonist addition (e.g., from 35 to 45% for clathrin), but the increase was not statistically significant (Fig. 2E). Immunogold labeling of ultrathin cryosections at the EM level confirmed that GAIP (small gold) is located on CCPs that also label for clathrin (Fig. 4A), AP-2 (Fig. 4, B and C), and dynamin (Fig. 4D). We also carried out labeling for caveolin-1α, a marker for caveolae (Anderson, 1998), but we were unable to detect caveolin in these cells. We conclude that in 293SDFDOR cells, as in other cell types (De Vries et al., 1998), GAIP is present on CCPs with clathrin, AP-2, and dynamin coats.

GAIP Does Not Traffic to Early Endosomes. After stimulation of DOR, CCVs containing the receptor bud from the PM and traffic to early endosomes (Tsao and von Zastrow, 2001). To determine whether GAIP also traffics to endosomes after receptor stimulation, we carried out double labeling for GAIP and EEA1, a marker for early endosomes (Mu et al., 1995). GAIP did not colocalize with EEA1 either before or 1 to 10 min after DPDPE addition (Fig. 3D). As a positive control, cells were allowed to take up Alexa Fluor-568 transferrin for 10 min; as expected, significant overlap was seen between transferrin and EEA1 (data not shown). Based on its consistent localization in CCPs and lack of overlap with EEA1, we conclude that GAIP does not traffic to early endosomes and remains associated with CCPs after agonist stimulation of DOR.

GAIP Colocalizes with DOR in dyn(K44A) Cells after Agonist Stimulation. DOR is located on the PM in 293SFDOR cells, and after agonist stimulation, it is phosphorylated (Murray et al., 1998) and traffics first to endosomes and then to lysosomes (Tsao and von Zastrow, 2000). To determine whether GAIP and DOR colocalize in the same

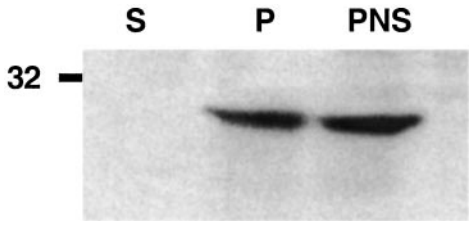

Fig. 1. Distribution of GAIP in cell fractions. GAIP is found exclusively in the membrane pellet (P) and is not detected in the supernatant or cytosolic fraction (S) prepared from a postnuclear supernatant (PNS) of 293SFDOR cells. Membrane (100,000*g* pellet) and cytosolic (100,000*g* supernatant) fractions were prepared from the postnuclear supernatant (PNS). The two fractions were normalized by volume as described under *Materials and Methods*, and proteins were separated by 12% SDS-PAGE and immunoblotted using anti-GAIP (N) (1:3000).

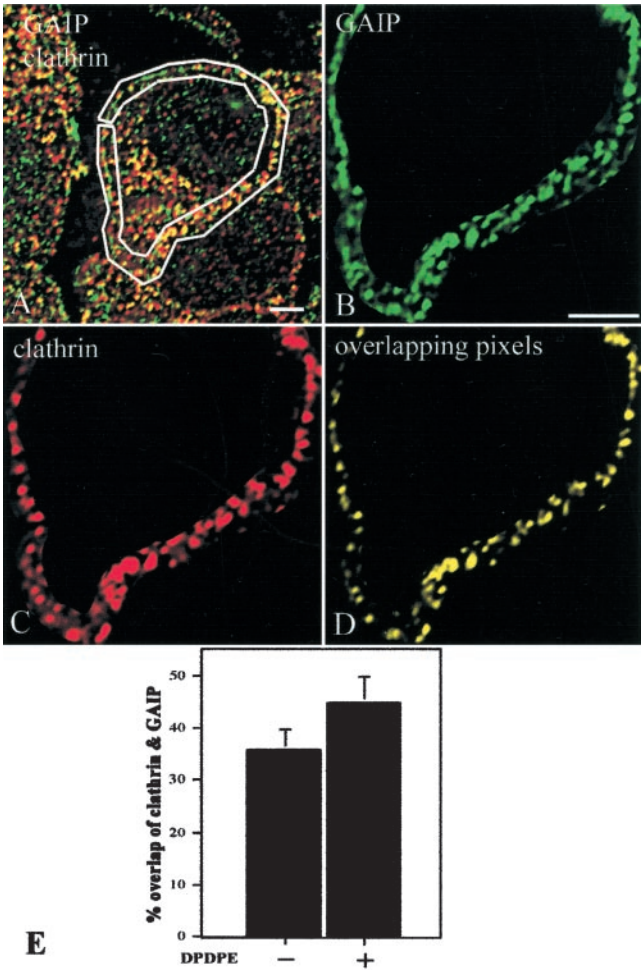

Fig. 2. Methods for semiquantitation of overlapping pixels obtained by deconvolution analysis. A, field from a merged deconvolution image of cells incubated with DPDPE for 1 min and double-stained for GAIP (green) and clathrin (red) showing overlap in their distribution (yellow dots). The cell membrane area used for quantification is traced in white. B to D, enlargement showing total pixels for GAIP, clathrin, and the overlapping pixels of the merged image in the traced area. E, graph showing summary of data obtained from cells (four each) incubated in the presence (+) or absence (−) of DPDPE and then processed, traced, and quantified as in A to D, Overlap in the distribution of GAIP and clathrin varies from 30 to 50%. There is a slight increase (from ~36 to ~45%) in overlap after agonist addition, but the increase is not statistically significant. 293SFDOR cells were incubated with or without DPDPE (1 min), fixed in 2% paraformaldehyde, and processed for immunofluorescence as described in detail under *Materials and Methods*. Cells were double-labeled with rabbit anti-GAIP (C) and mouse anti-clathrin mAb followed by Alexa Fluor-488 goat anti-rabbit and Alexa Fluor-594 goat anti-mouse F(ab′)2. Images were captured by deconvolution microscopy. Cell membrane areas were traced using Photoshop 5.5 and total GAIP pixels (green), clathrin pixels (red), and those positive for both GAIP and clathrin (yellow) within the traced area were measured using NIH Image software. The percentage of the total GAIP pixels that overlap with clathrin pixels in the PM region was then determined, and average and S.D. were calculated. Scale bars, 2.5 μm.

CCPs, we carried out double labeling for GAIP and FLAG-DOR. GAIP and FLAG-DOR did not overlap significantly (<5%) either before or after addition of DPDPE for 1 min (Fig. 3, E-G). Similarly, no colocalization was observed at 3, 5, or 10 min after addition of agonist (data not shown).

We reasoned that because it takes <1 min for a CCV to form and bud (Marsh and McMahon, 1999), it might be difficult to capture the colocalization of DOR and GAIP in CCPs if their codistribution is transient. To inhibit or slow down the budding process, we transfected cells with dominant-negative dyn(K44A), a dynamin mutant that inhibits budding of CCVs, thereby trapping CCVs at the cell surface and inhibiting receptor internalization (Damke et al., 1994). In the absence of agonist, little or no (<5%) overlap was found between GAIP and DOR in dyn(K44A)-transfected cells; however, 30 min after adding DPDPE, a striking overlap was observed in coated pits located along the PM (Fig. 3, H–J). The percentage overlap increased from <5 to ~45% after agonist addition (Fig. 5). From these data, we conclude that upon binding agonist, DOR moves from noncoated regions of the PM into CCPs with GAIP; the process is so rapid that it cannot be detected unless it is slowed down or synchronized by expressing dyn(K44A), which produces "frozen" intermediates.

We attempted to carry out double immunogold labeling for FLAG-DOR at the EM level but were unsuccessful. To validate the effectiveness of dyn(K44A) expression we carried out routine EM on 293SFDOR cells expressing dyn(K44A) and on controls. In nontransfected cells individual coated pits and vesicles were scattered along the PM (Fig. 6A). By contrast, in cells expressing dyn(K44A) groups of CCPs (Fig. 6, B–E) or those in continuity with other vesicles (Fig. 6, D–E) or long tubular structures in continuity with the PM were commonly seen (Fig. 6, C and F). Some of these vesicles showed typical dynamin rings at their elongated necks (Fig. 6, B, E, F) comparable with those described previously in dyn(K44A)-transfected cells (Damke et al., 1994; Baba et al., 1999).

GAIP Colocalizes with Gαi3-YFP after Agonist Binding to DOR. We have shown previously that when Gαi3-YFP is expressed in COS cells, it is correctly targeted to the PM and Golgi membranes (Weiss et al., 2001). To determine where the interaction between GAIP and Gαi3 takes place after stimulation of DOR, we expressed Gαi3-YFP (Weiss et al., 2001) in 293SFDOR cells, labeled the cells for endogenous

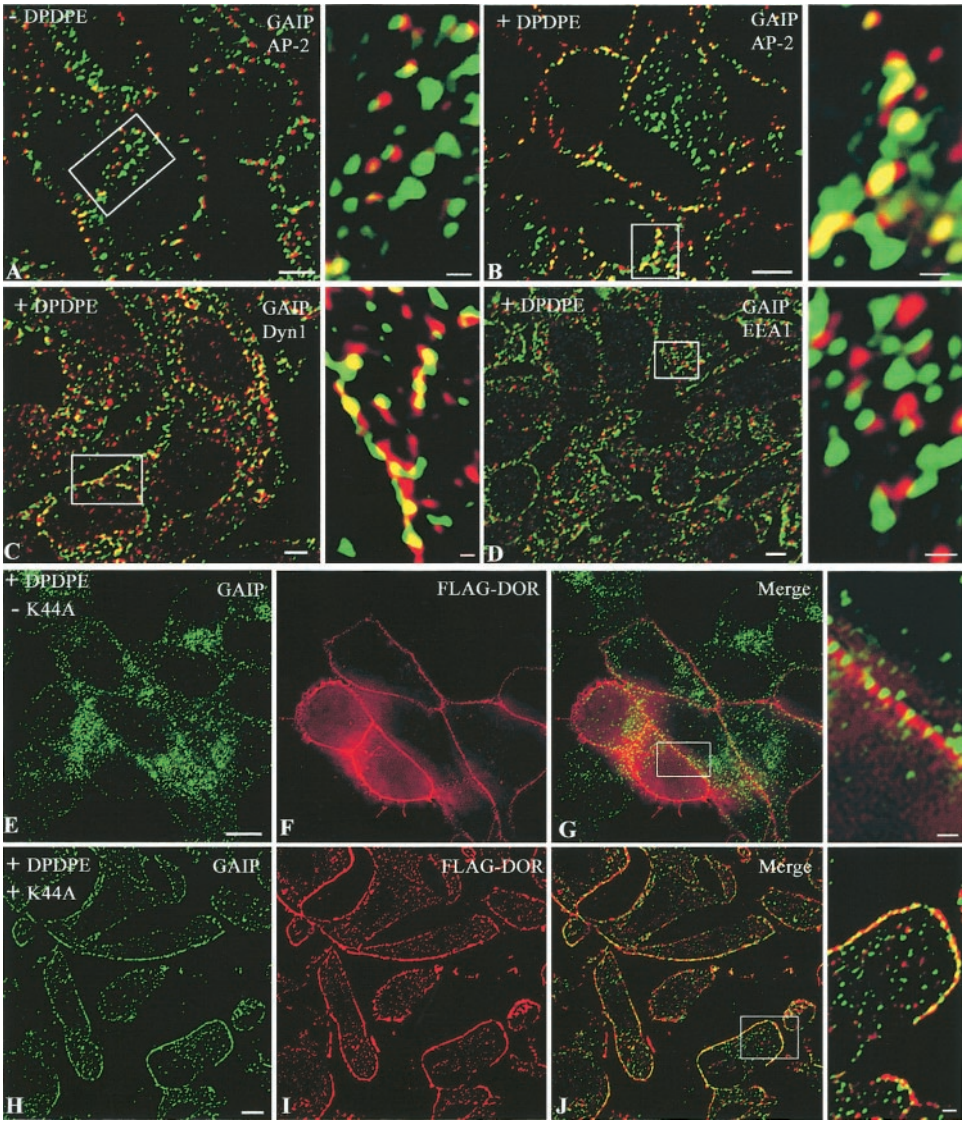

Fig. 3. GAIP is localized in clathrin-coated pits. A and B, colocalization (yellow dots) of endogenous GAIP (green) and AP-2 (red) in the absence (−DPDPE) or presence (+DPDPE) of agonist. C, colocalization (yellow dots) of GAIP (green) with dynamin (red). D, the distribution of GAIP (green) and the endosome marker, EEA-1 (red), does not overlap after agonist treatment (10 min). E to G, little or no overlap is seen in staining of GAIP (green, E) with DOR-FLAG (red, F) after DPDPE addition (1 min). G is the merged image. H to J, in cells expressing mutant dynamin (+K44A), there is a striking overlap (yellow dots in merged image) in the distribution of GAIP and DOR-FLAG at the PM 30 min after DPDPE addition. Whole cells (E–G) or semithin cryosections (A–D, H–J) prepared from parental 293SFDOR cells (A–G) or those expressing dyn(K44A) (H–J) were processed for immunofluorescence as in Fig. 2 and incubated with rabbit anti-GAIP (C) and mouse AP-2, EEA1, or FLAG (M2) followed by incubation with Alexa Fluor-488 goat anti-rabbit and Alexa Fluor-594 goat anti-mouse $F(ab')_2$ and analysis by deconvolution microscopy. Boxes indicate enlarged areas. Scale bars, 2.5 μm; scale bars in boxed areas, 1 μm.

GAIP and Gαi3-YFP (with a GFP antibody), and carried out deconvolution analysis (Fig. 7, A–D) and quantification of overlapping pixels (Fig. 7H) before and after agonist binding. In the absence of agonist, GAIP showed its usual punctate distribution in CCPs, whereas Gαi3-YFP showed a more uniform linear distribution along the PM (Fig. 7A). Relatively little (~10%) overlap in their distribution was seen along the PM. As reported previously, Gαi3-YFP was also found in CCPs concentrated in the Golgi region (Weiss et al., 2001). After DPDPE addition (1 min), overlap between GAIP and Gαi3-YFP at the PM was significantly increased (to 30%) (Fig. 7, B and H). In dyn(K44A)-transfected cells, there was also little overlap (10%) at the PM before adding agonist (Fig. 7, C and H), but after agonist addition, the majority of the GAIP (65%) at the PM colocalized with Gαi3-YFP (Fig. 7, D and H). These results demonstrate that Gαi3-YFP and GAIP, for the most part, do not codistribute on the PM before agonist addition; upon agonist binding Gαi3-YFP, DOR, and/or GAIP are able to move, redistribute within the PM and colocalize in both parental and dyn(K44A)-expressing cells.

GAIP Is Localized on Clathrin/AP-2 Coated Pits and Gαi3 on Noncoated Microdomains of the PM. The above results raised the question of where GAIP and Gαi3-YFP meet—i.e., in CCPs, where GAIP is located, or on non–clathrin-coated regions of the PM, where Gαi3-YFP is found at steady state. When double immunofluorescence labeling for Gαi3-YFP with AP-2 was performed, little (~5%) or no overlap was detected in their distribution along the PM (Fig. 7E), but overlap increased slightly (20%) after agonist binding (Fig. 7I). Similarly, in dyn(K44A) transfected cells, there was little or no overlap (~5%) between Gαi3-YFP and AP-2 stain-

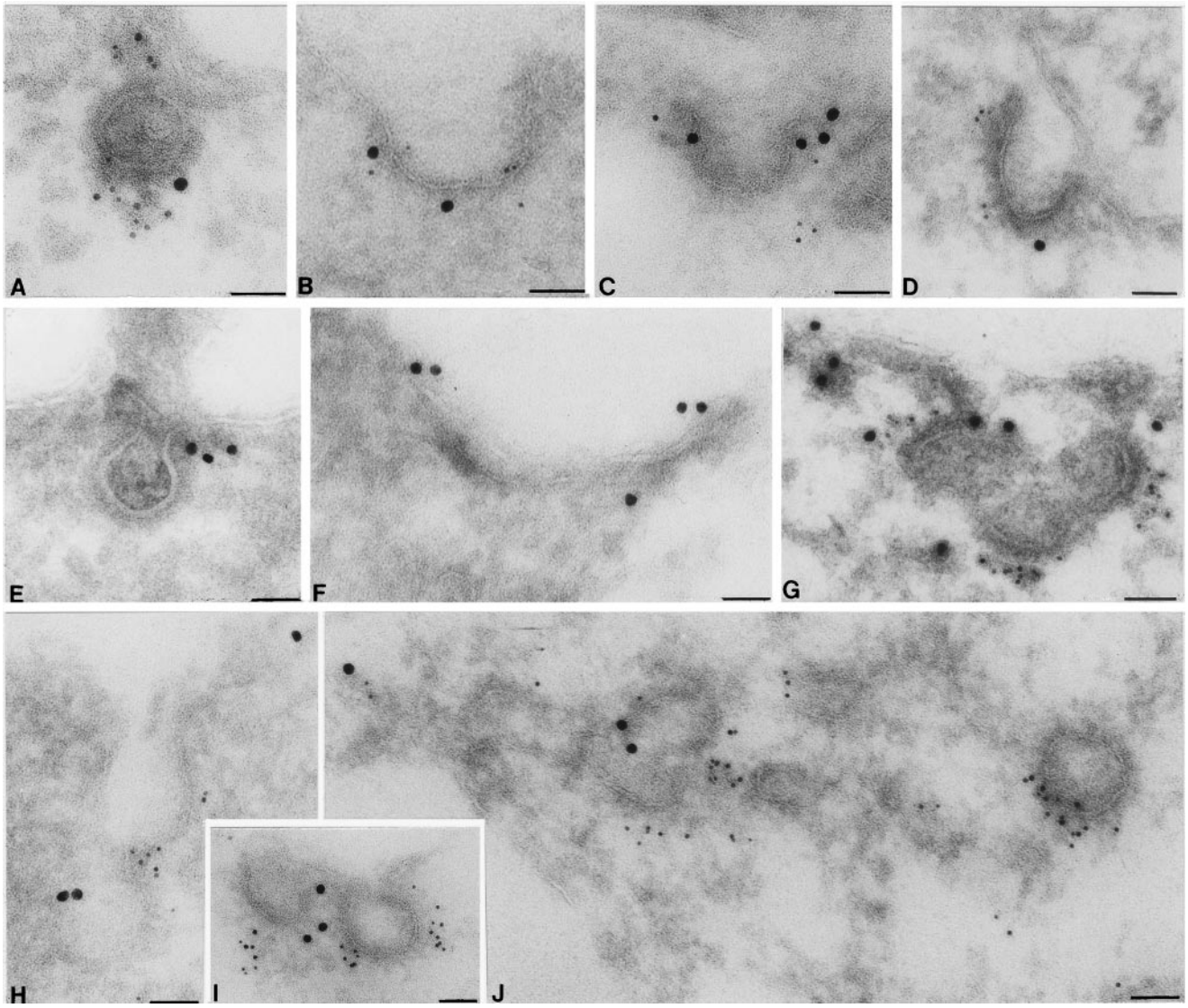

Fig. 4. Immunogold labeling demonstrating colocalization of GAIP (small gold) with coated pit markers and G proteins along the PM. A to D, GAIP is found on the same vesicles as clathrin (A), AP-2, (B and C), and dynamin (D) (large gold). E and F, labeling for Gαi3-YFP (E) and Gβ (F) subunits is concentrated at the necks of CCPs. G to I, GAIP colocalizes with dynamin (G and I) and clathrin (H) on the same CCPs in dyn(K44A)-transfected cells 30 min after agonist addition. J, GAIP colocalizes with Gαi3-YPF on clusters of CCVs 30 min after agonist stimulation in dyn(K44A)-transfected cells. Parental cells (A–F) or dyn(K44A)-transfected cells (G–J) were stimulated with DPDPE for 1 min or 30 min, respectively, and processed for ultrathin cryosectioning. Sections were either labeled for Gαi3-YFP (rabbit anti-GFP) (E) or rabbit Gβ (F) or double-labeled with rabbit anti-GAIP (5 nm gold) and mouse anti-clathrin heavy chain (A, H), anti-AP-2 (B–C), anti-dynamin (D, I), or anti-HA-dynamin (10 nm gold) (G) followed by goat anti-rabbit IgG conjugated to 5 nm gold and goat anti-mouse IgG conjugated to 10 nm gold. Scale bar, 0.05 μm.

ing along the PM in the absence of agonist; however, after addition of agonist, there was a striking overlap (>60%) between staining for Gαi3-YFP and AP-2 (Fig. 7, F and I) along the PM. Instead of direct superimposition of red and green dots, there was only partial overlap at the edges of the dots, suggesting that G proteins are located near CCPs. Interestingly, the distribution of Gβγ subunits did not overlap with AP-2 either before or after agonist addition (Fig. 7G), suggesting that Gαi3-YFP disassociates from Gβγ subunits that remain associated with non–clathrin-coated regions of the PM after agonist binding.

After immunogold labeling, Gαi3-YFP (Fig. 4E) and Gβ (Fig. 4F) were found all along the PM but were often clustered at the neck of CCPs and were not usually seen deeper in CCPs either before or after agonist addition. From these results, we conclude that Gαi3 and Gβγ subunits are located on noncoated microdomains of the PM at steady state; for GAIP and Gαi3 to interact after G protein activation, Gαi3 must move into CCPs together with DOR. In dyn(K44A)-transfected cells, Gαi3-YFP was also confined mainly to the neck of the CCPs after agonist stimulation (Fig. 4J). By contrast, GAIP (Fig. 4, G–J), clathrin (Fig. 4H), AP-2, and dynamin (Fig. 4I) were detected all around the coated pits in both nontransfected cells (Fig. 3, A–F) and those transfected with dyn(K44A) (Fig. 4, G–I).

Taken together, these findings indicate that GAIP, clathrin, AP-2, and dynamin are localized around the entire perimeter of coated pits, whereas Gαi3-YFP and Gβγ are located in noncoated regions of the PM and may be concentrated at the neck of coated pits. We speculate that upon agonist binding, GAIP and Gαi3 meet at the neck of the CCPs.

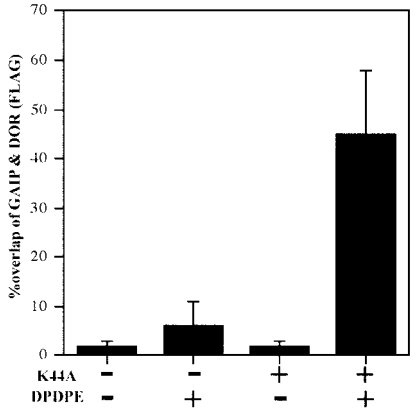

Fig. 5. Semiquantitation of overlapping pixels obtained by deconvolution analysis of GAIP and FLAG-DOR. There is little overlap (<5%) in the distribution of GAIP and FLAG-DOR in either the presence or absence of agonist in nontransfected cells (−K44A). However, in cells transfected with the dynamin mutant (+K44A), there is a dramatic increase (to ~45%) in the amount of overlap after adding agonist indicating that DOR are trapped in CCPs containing GAIP. 293SFDOR cells were transfected (+K44A) or not (−K44A) with mutant dynamin and incubated in the absence (−) or presence (+) of DPDPE for 30 min and fixed and processed for immunofluorescence as described under *Materials and Methods*. Cells were doubly incubated with rabbit anti-GAIP (C) and mouse anti-FLAG (M2) followed by Alexa Fluor-488 goat anti-rabbit and Alexa Fluor-594 goat anti-mouse $F(ab')_2$ and analysis by deconvolution microscopy. Plasma membranes areas were traced, total GAIP pixels (green), FLAG pixels (red), and those positive for both GAIP and FLAG (yellow) within the traced area were calculated, and the percentage of the total GAIP that overlaps with FLAG-DOR in the PM region was then determined and average and S.D. was calculated as for Fig. 2.

GAIP and Gαi3 Form a Coprecipitable Protein Complex. Our immunofluorescence data indicated that GAIP, Gαi3-YFP, and DOR colocalize in CCPs, suggesting that GAIP could bind to Gαi3 in this location. To determine whether Gαi3 and GAIP interact in CCPs in vivo, we expressed GAIP, Gαi3-YFP, and dyn(K44A) in 293SFDOR cells and carried out immunoprecipitation with an anti-GFP mAb on membrane and cytosolic fractions followed by immunoblotting for GAIP. We found that GAIP could be coimmunoprecipitated with Gαi3-YFP from membrane fractions (Fig. 8, lanes 5–6) but not from cytosolic fractions (Fig. 8, lanes 3–4). Moreover, GAIP was detected in immunoprecipitates obtained from both stimulated and unstimulated (with DPDPE) cells. These results support our conclusion that the interaction between GAIP and Gαi3-YFP takes place in CCPs and indicate that the interaction is stable enough to resist detergent extraction and immunoprecipitation. The explanation for our finding that GAIP is coimmunoprecipitated in

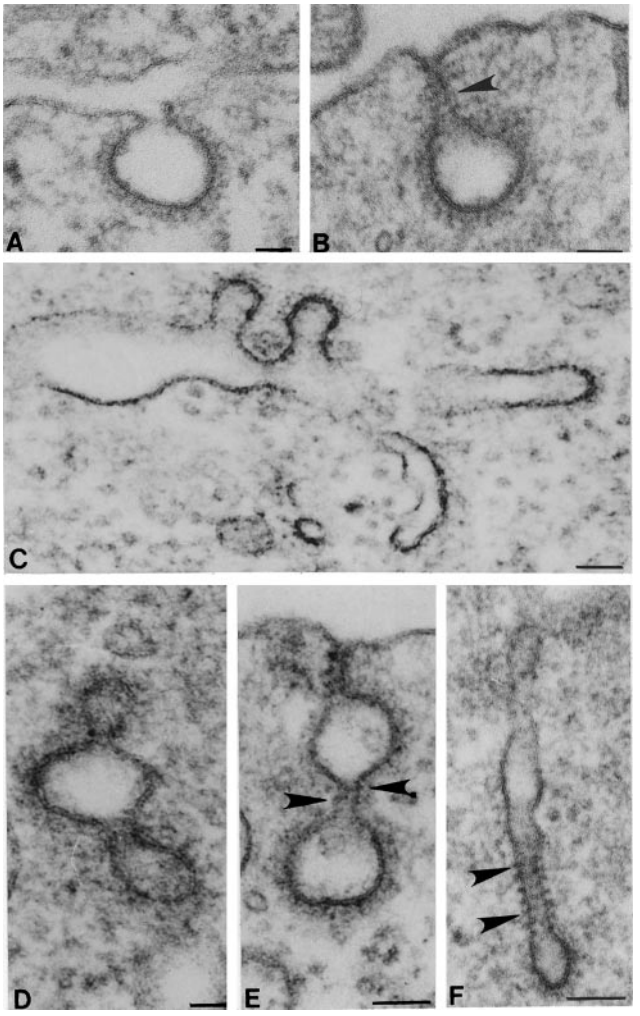

Fig. 6. Expression of dyn(K44A) leads to the accumulation of CCPs in continuity with invaginations of the PM in 293SFDOR cells. A, nontransfected cell showing the usual topography of an individual CCP at the PM. B to F, Dyn(K44A) transfected cells showing accumulation of clusters of CCPs with a variety of shapes and conformations. Some (E) resemble an hourglass, others (B, E, F) bud from deep invaginations of the PM, and many (B, E, F) have typical dynamin necklaces (arrows). Nontransfected cells (A) or cells transfected with dyn(K44A) (B–F) were processed for routine EM. In B to F, DPDPE was added for 30 min at 24 h after transfection. Scale bar, 0.05 μm.

both the presence and absence of agonist remains to be determined.

Discussion

The purposes of this study were to determine GAIP's site of interaction with Gαi3 and GAIP's fate after agonist stimulation of DOR, a Gαi-linked GPCR. Our major findings are that: 1) endogenous GAIP does not colocalize with Gαi3-YFP and DOR at the PM before agonist addition, whereas after adding agonist, Gαi3-YFP and DOR redistribute on the PM and colocalize with GAIP in CCPs; 2) GAIP remains associated with CCPs at the PM, whereas DOR is internalized in CCVs; and 3) DOR but not GAIP traffics to early endosomes. We also found that when DOR is stimulated with agonist and endocytosis is blocked with dyn(K44A), GAIP, Gαi3-YFP, and DOR colocalize on the same CCPs, indicating that Gαi3 moves into CCPs, where it encounters GAIP, which is stably associated with CCPs. Moreover, we found that when GAIP and Gαi3-YFP are cotransfected into cells stably expressing DOR, GAIP and Gαi3-YFP can be coimmunoprecipitated, suggesting that they form a detergent-resistant protein complex.

Based on our findings, we hypothesize the following model for the fate of GAIP after agonist stimulation of DOR (Fig. 9): 1) before agonist stimulation, GAIP is found on clathrin-coated microdomains, whereas DOR and Gαi3 (GDP) are found on noncoated regions of the PM; 2) after addition of agonist, DOR binds and activates Gαi3, which dissociates from Gβγ subunits, and the DOR/Gαi3(GTP) complex moves within the plane of the PM to bind GAIP at the neck of a CCP. The Gβγ subunits remain behind on noncoated microdomains. GAIP acts as a GAP, returning Gαi to its GDP-bound form, and then dissociates from Gα. Gα redistributes back to

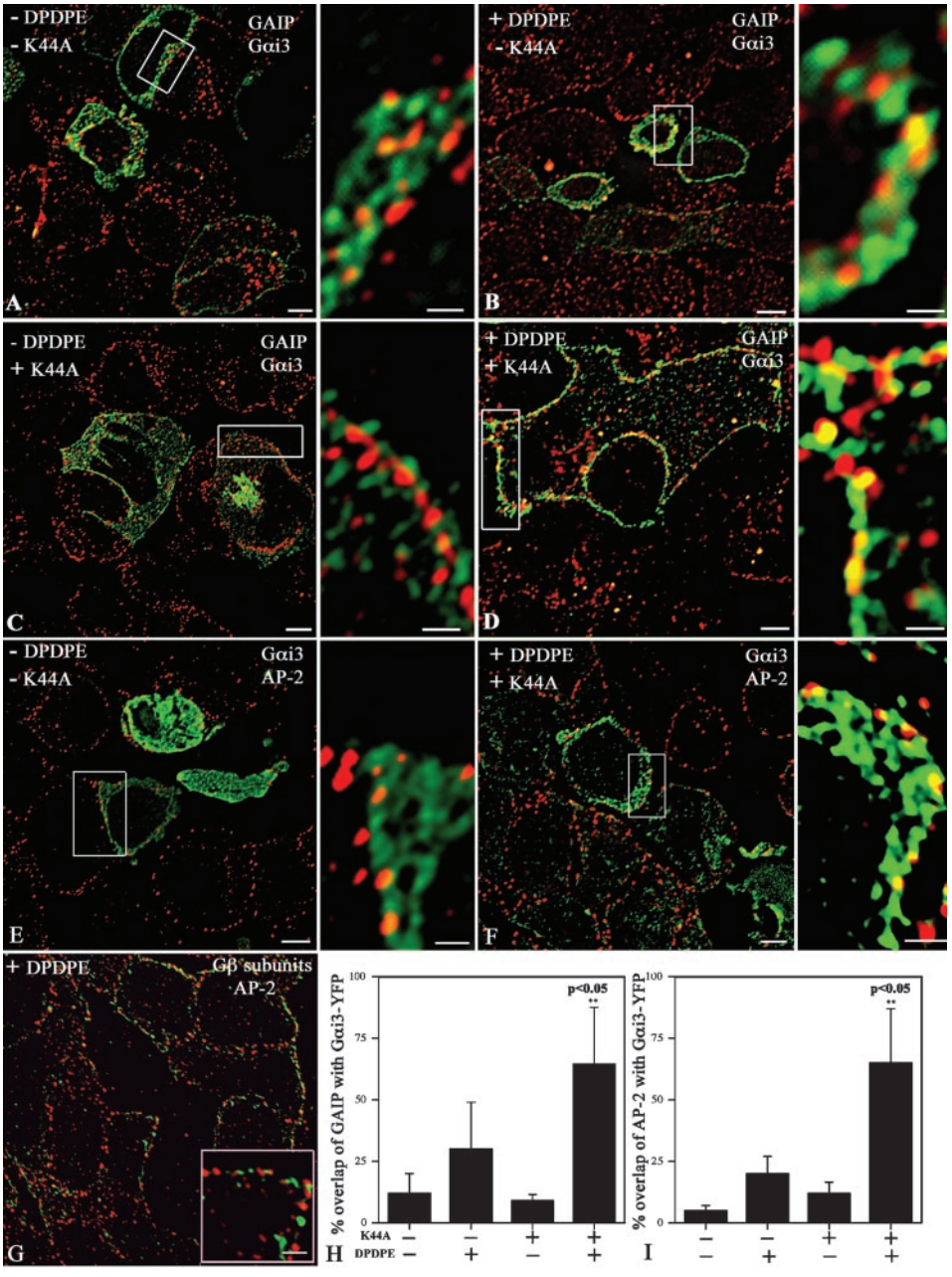

Fig. 7. Redistribution of Gαi3-YFP to CCPs after agonist addition. A, before agonist addition, there is relatively little overlap in the distribution of GAIP (red) and Gαi3-YFP (green) along the PM. B, immediately (1 min) after addition of DPDPE, overlap between GAIP (red) and Gαi3-YFP (green) is increased as indicated by the yellow dots. C, there is also little overlap in the distribution of GAIP and Gαi3-YFP before agonist addition in dyn(K44A) transfected cells. D, after adding agonist (30 min) the majority of the GAIP on the PM partially colocalizes with Gαi3-YFP in dyn(K44A) transfected cells. E, in dyn(K44A) transfected cells relatively little Gαi3-YFP (green) colocalizes with AP-2 (red) along the PM before agonist stimulation. F, after stimulation with DPDPE for 30 min, there is a dramatic increase in the overlap between of Gαi3-YFP (green) and AP-2 (red) along the PM in dyn(K44A) transfected cells, as most of the red dots along the PM colocalize in part with Gαi3. Note that there is only partial superimposition (yellow) of staining for Gαi3-YFP (green dots) and clathrin (red dots), suggesting close proximity but incomplete overlap. G, no overlap is seen in the distribution of Gβ (green) subunits and AP-2 (red) in dyn(K44A) transfected cells stimulated for 30 min. H, bar graph showing results of quantification of overlapping pixels in the PM region in cells doubly labeled for GAIP and Gαi3-YFP. After DPDPE addition, the percentage overlap of total GAIP pixels with Gαi3-YFP pixels increased from 10 to 30%; in cells expressing dynamin mutant (+K44A), overlap increased dramatically from ~5 to 60% after agonist addition. I, similar bar graph showing results of quantification of overlapping pixels in the PM region in cells doubly labeled for Gαi3-YFP and AP-2. Overlap of Gαi3-YFP with total AP-2 pixels increases dramatically from ~10 to 65% 30 min after agonist addition to dyn(K44a)-transfected 293SFDOR cells. Semithin cryosections were processed as in Fig. 2, double-labeled using mouse anti-GFP mAb and either rabbit anti-GAIP (C), AP-2, or mouse AP-2 and rabbit anti-Gβ followed by Alexa Fluor-594 goat anti-mouse and Alexa Fluor-488 goat anti-rabbit F(ab′)$_2$. The percentage of overlap of red and green pixels (PM only) was determined as for Fig. 2. At least five cells per treatment were analyzed to obtain averages and S.D. Scale bars, 2.5 μm; scale bars in boxed areas, 1 μm.

non–clathrin-coated microdomains of the PM and reassociates with the G$\beta\gamma$ complex. 3) The receptors cluster in the CCP, a CCV containing DOR starts to bud from the CCP, and dynamin translocates from the cytosol to the budding CCV. GAIP remains stably associated with clathrin-coated microdomains of the PM. 4) The CCV containing DOR separates from the PM, loses its clathrin coat, and traffics to early endosomes and subsequently to lysosomes, where the receptor is degraded (Tsao and von Zastrow, 2000).

This represents a novel paradigm for spatial regulation of G protein signaling through stable association of a GAP with a specific type of membrane microdomain. The extent to which this paradigm is unique for GAIP or applies to other RGS proteins is unknown. However, most RGS proteins have been shown to be present in both membrane and cytosolic pools and several—i.e., mammalian RGSZ1, RGS3, RGS4, RGS7, RGS9, and yeast *Sst*2—have been shown to be membrane bound and or to translocate to specific membrane compartments upon G protein activation. Therefore, it seems likely that this paradigm might apply to at least some other RGS proteins. In the cell, this would have the advantage of allowing for functional specificity of individual RGS proteins by addressing them to specific subcellular sites.

It should be stressed that both GAIP (De Vries et al., 1998) and Gαi3 (Weiss et al., 2001) are located on intracellular (i.e., Golgi) membranes as well as the cell membrane. Our model is based on the behavior of PM-associated GAIP, but we assume that similar interactions occur in the Golgi, where the functions of Gαi3 remain largely unknown (De Vries et al., 2000).

The above model rests on the assumption that GAIP remains stably associated with CCVs after agonist stimulation. An alternative but less likely possibility is that GAIP is released from CCVs into the cytosol after binding Gαi3. However, this scenario would require removal of GAIP's lipid anchor, because GAIP is anchored to membranes via palmitoylation (De Vries et al., 1996). This seems unlikely; if GAIP were constantly dissociating from CCVs, we would expect to detect it in the cytosol, which is not the case. GAIP is entirely membrane bound in 293SFDOR cells.

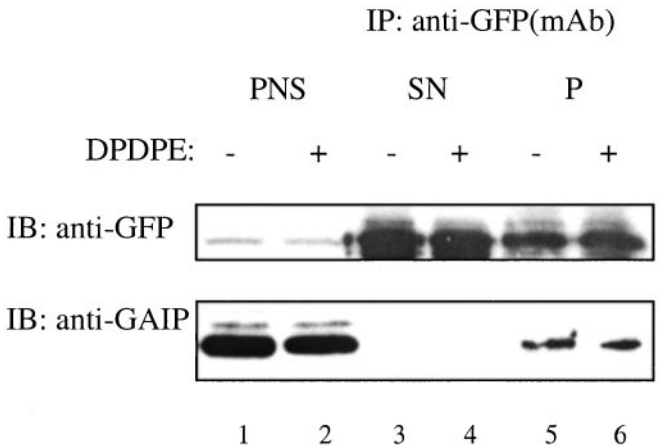

Fig. 8. Gαi3 and GAIP form a coimmunoprecipitable protein complex. A, PCDNA3-GAIP, pCDNA3-Gαi3-YFP, and pCB-K44A-dyn were transiently transfected into 293SFDOR cells that stably express DOR. Cells were then stimulated with 5 μm DPDPE (lanes 2, 4, and 6), after which they were homogenized and membrane (100,000*g* pellet) and soluble (100,000*g* supernatant) fractions were prepared from a postnuclear supernatant (PNS) as in Fig. 1. Immunoprecipitation (IP) was carried out on both supernatant (SN) and pellet (P) fractions with anti-GFP mAb; the precipitated proteins were then separated by SDS-PAGE and immunoblotted using anti-GAIP or anti-GFP. GAIP is detected in the IP obtained from the membrane pellet (lanes 5 and 6) but not in the IP obtained from the supernatant (lanes 3 and 4). Lanes 1 and 2, immunoblots of PNS showing the total GAIP and Gαi3-YFP in the PNS. The amount of protein loaded was 2% of that used for immunoprecipitation.

Our data imply that rather than a single CCV forming from a single coated pit, CCVs can bud from clathrin-coated microdomains that are stably associated with the PM. GAIP represents a marker for at least one type of stable microdomain (i.e., the sites from which the Gαi-linked receptor DOR buds). This is consistent with previous findings suggesting that CCVs bud from stable coated pits (Jin and Nossal, 1993). Moreover, using GFP-tagged clathrin light chain, it was observed that coated pit fluorescence frequently persists after the emergence of one or multiple CCVs, suggesting that CCVs bud from stable clathrin-coated sites on the PM (Gaidarov et al., 1999).

It is of interest that GAIP and Gαi3-YFP do not colocalize before ligand stimulation but are able to redistribute within the PM and to colocalize in CCPs after agonist binding in both parental and dyn(K44A)-expressing cells. We did not see colocalization of DOR and GAIP in parental cells after ligand binding, probably because the internalization process is very rapid; the entire process of vesicle formation and budding from the PM takes less than a minute (Marsh and McMahon, 1999). By slowing internalization with dyn(K44A) and producing "frozen" intermediates, it was possible to catch GAIP, Gαi3-YFP, and DOR in the same CCPs at the PM. Dyn(K44A) expression has been shown to trap CCVs at the cell surface (Damke et al., 1994) and thereby to block endocytosis of DOR (Keith et al., 1996) as well as the transferrin receptor and a number of other GPCRs (Gargnon et al., 1998; Heding et al., 2000; Hinshaw, 2000).

There has been considerable debate concerning whether components of G protein signaling complexes are restricted in their distribution to specific domains of the PM or are able to diffuse freely (Neubig, 1994; Steinberg and Brunton, 2001). Our results provide evidence for a novel paradigm for spatial regulation of G protein signaling by restricting the distribution of the RGS protein GAIP to specific clathrin-coated microdomains, whereas GPCR and Gαi are able to move in and out of clathrin- and non–clathrin-coated microdomains of the PM. G proteins have been assumed to remain associated with the PM after agonist stimulation (Wedegaertner, 1998; Hughes et al., 2001). A potential exception is Gαs; evidence has been obtained that it leaves the PM and is either released into the cytosol (Wedegaertner et al., 1996) or internalized (Yu and Rasenick, 2002) after receptor and G protein activation.

Recent studies have documented that G proteins (Shaul and Anderson, 1998), as well as some signaling molecules, are present in caveolae or lipid rafts, which represent cholesterol and sphingolipid-rich microdomains of the PM (Simons and Toomre, 2000; Ikonen, 2001), and it has been suggested that lipid rafts act as organizing centers for GPCR signal transduction. However, the majority of Gαi subunits are not associated with lipid rafts (Miotti et al., 2000; Moffett et al., 2000), and most signaling molecules are associated with both raft and nonraft regions of membranes as defined by detergent-insolubility. In fact, there is now increasing evidence that signaling molecules and receptors, including

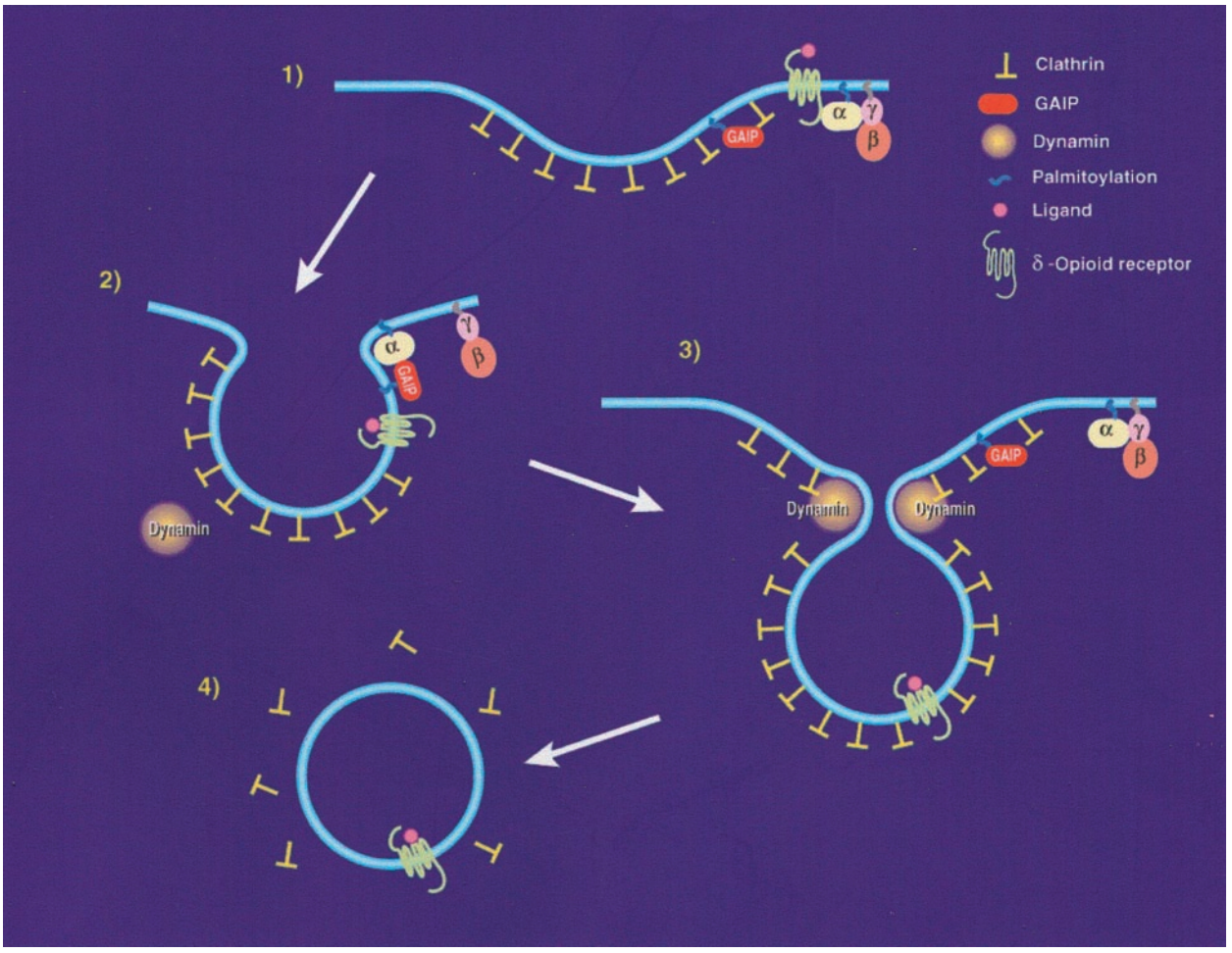

Fig. 9. Model for GAIP's fate after stimulation of DOR. 1, at resting state GAIP is localized on CCPs of the PM, whereas DOR and inactive Gαi/βγ trimers are on noncoated regions of the PM. 2, after agonist addition, activated (GTP-bound) Gαi and Gβγ subunits separate and signal to their downstream effectors, and Gαi3 and DOR move toward the clathrin-coated microdomain and bind GAIP at the neck of the CCP. GAIP acts as a GAP for Gαi returning Gαi3 to its inactive, GDP-bound form. 3, Gαi3 moves away from the CCP and reassociates with the Gβγ subunits in non–clathrin-coated domains of the PM. A CCV containing DOR starts to bud from the CCP, and dynamin translocates from the cytosol to the neck of the nascent CCV. GAIP remains on the CCP. 4, the CCV containing DOR buds from the PM, loses its clathrin coat, and traffics to endosomes and onto lysosomes (not shown), where DOR is degraded (Tsao and von Zastrow, 2000).

GPCR (Steinberg and Brunton, 2001) can move from lipid rafts to nonraft domains and back again, and others can cluster in lipid rafts and diffuse in the plane of the membrane to be internalized via CCVs. For example, at resting state, the EGF receptor is concentrated in caveolae; upon EGF binding, the receptor exits caveolae, migrates to noncaveolar domains of the PM and is internalized in CCVs (Anderson, 1998). Similarly, both cholera (Shogomori and Futerman, 2001) and Shiga toxins (Katagiri et al., 1999) are found in lipid rafts at the PM and are internalized in CCVs. Interestingly, cholesterol has been shown to be a component of coated pits as well as caveolae, and cholesterol depletion inhibits CCV budding (Rodal et al., 1999; Subtil et al., 1999) raising the possibility that cholesterol-rich lipid rafts may be present in CCPs and might serve to separate signaling components within different parts of the coated pit. Further research is needed to determine whether lipid rafts (which may be as small as 20 nm) exist within coated pits and to establish the mechanism by which GAIP remains on coated pits while DOR is internalized in CCVs.

Acknowledgments

We thank Dr. Scott Emr (Howard Hughes Medical Research Institute, University of California San Diego) for the use of his deconvolution microscope. Some of the deconvolution images were collected in the Digital Imaging Shared Resource Core of the Rebecca and John Moores University of California San Diego Cancer Center.

References

Anderson RGW (1998) The caveolae membrane system. *Annu Rev Biochem* **67:**199–225.

Baba T, Ueda H, Terada N, Fujii Y, and Ohno S (1999) Immunocytochemical study of endocytic structures accumulated in HeLa cells transformed with a temperature-sensitive mutant of dynamin. *J Histochem Cytochem* **47:**637–648.

Brodsky FM, Chen CY, Knuehl C, Towler MC, and Wakeham DE (2001) Biological basket weaving: formation and function of clathrin-coated vesicles. *Annu Rev Cell Dev Biol* **17:**517–568.

Damke H, Baba T, Warnock DE, and Schmid SL (1994) Induction of mutant dynamin specifically blocks endocytic coated vesicle formation. *J Biol Chem* **127:**915–934.

De Vries L, Bin Z, Fischer T, Elenko E, and Farquhar MG (2000) The regulator of G protein signaling family. *Annu Rev Pharmacol Toxicol* **40:**235–272.

De Vries L, Elenko E, Hubler L, Jones TL, and Farquhar MG (1996) GAIP is membrane-anchored by palmitoylation and interacts with the activated (GTP-bound) form of Gαi subunits. *Proc Natl Acad Sci USA* **93:**15203–15208.

De Vries L, Elenko E, McCaffery JM, Fischer T, Hubler L, McQuistan T, Watson N, and Farquhar MG (1998) RGS-GAIP, a GTPase-activating protein for Gαi heterotrimeric G proteins, is located on clathrin-coated vesicles. *Mol Biol Cell* **9:**1123–1134.

De Vries L, Mousli M, Wurmser A, and Farquhar MG (1995) GAIP, a protein that specifically interacts with the trimeric G protein Gαi3, is a member of a protein family with a highly conserved core domain. *Proc Natl Acad Sci USA* **92:**11916–11920.
Ferguson SSG (2001) Evolving concepts in G protein-coupled receptor endocytosis: the role in receptor desensitization and signaling. *Pharmacol Rev* **53:**1–24.
Fishburn CS, Pollitt SK, and Bourne HR (2000) Localization of a peripheral membrane protein: Gβγ targets $G\alpha_Z$. *Proc Natl Acad Sci USA* **97:**1085–1090.
Gaidarov I, Santini F, Warren RA, and Keen JH (1999) Spatial control of coated-pit dynamics in living cells. *Nat Cell Biol* **1:**1–7.
Gargnon AW, Kallal L, and Benovic JL (1998) Role of clathrin-mediated endocytosis in agonist-induced down-regulation of the β_2-adrenergic receptor. *J Biol Chem* **273:**6976–6981.
Heding A, Vrel M, Hanyalgolu AC, Sellar R, Taylore PL, and Eidne KA (2000) The rat gonadotropin-releasing hormone receptor internalizes via a beta-arrestin independent, but dynamin-dependent, pathway: addition of a carboxyl-terminal tail confers beta-arrestin dependency. *Endocrinol* **141:**299–306.
Hinshaw JE (2000) Dynamin and its role in membrane fission. *Annu Rev Cell Dev Biol* **16:**483–519.
Huang C, Hepler JR, Chen LT, Gilman AG, Anderson RG, and Mumby SM (1997) Organization of G proteins and adenylyl cyclase at the plasma membrane. *Mol Biol Cell* **8:**2365–2378.
Hughes TE, Zhang H, Logothetis DE, and Berlot CH (2001) Visualization of a functional $G\alpha_q$-green fluorescent protein fusion in living cells. *J Biol Chem* **276:**4227–4235.
Ikonen E (2001) Roles of lipid rafts in membrane transport. *Curr Opin Cell Biol* **13:**470–477.
Jin A and Nossal R (1993) Topological mechanisms involved in the formation of clathrin-coated vesicles. *Biophys J* **65:**1523–1537.
Katagiri YU, Mori T, Nakajima MT, Katagiri C, Taguchi T, Takeda T, Kiyokawa N and Fujimoto J (1999) Activation of Src family kinase Yes induced by shiga toxin binding to globotriaosyl ceramide (Gb3/CD77) in low density, detergent-insoluble microdomains. *J Biol Chem* **274:**35278–35282.
Keith DE, Murray SR, Zaki PA, Chu PC, Lissini DV, Kang L, Evans CJ, and von Zastrow M (1996) Morphine activates opioid receptors without causing their rapid internalization. *J Biol Chem* **271:**19021–19024.
Levis M and Bourne H (1992) Activation of the alpha subunit of Gs in intact cells alters its abundance, rate of degradation and membrane avidity. *J Cell Biol* **119:**1297–1307**.**
Marsh M and McMahon HT (1999) The structural era of endocytosis. *Science (Wash DC)* **285:**215–219.
Miotti S, Bagnoli M, Tomassetti A, Colnaghi MI, and Canevari S (2000) Interaction of folate receptor with signaling molecules lyn and $G\alpha_{i3}$ in detergent-resistant complexes from ovary carcinoma cell line IGROV1. *J Cell Sci* **113:**349–357.
Moffett S, Brown DA, and Linder ME (2000) Lipid-dependent targeting of G proteins into rafts. *J Biol Chem* **275:**2191–2198.
Mu FT, Callaghan JM, Steele-Mortimer O, Stenmark H, Parton RG, Campbell PL, McCluskey J, Yeo JP, Tock EP, and Toh BH (1995) EEA1, an early endosome-associated protein. EEA1 is a conserved α-helical peripheral membrane protein flanked by cysteine "fingers" and contains a calmodulin-binding IQ motif. *J Biol Chem* **270:**13503–13511.
Murray SR, Evans CJ, and von Zastrow M (1998) Phosphorylation is not required for dynamin-dependent endocytosis of a truncated mutant opioid receptor. *J Biol Chem* **273:**24987–24991.
Neubig RR (1994) Membrane organization in G-protein mechanisms. *Faseb J* **8:**939–946.
Rodal SK, Skretting G, Garred O, Vilhardt F, Deurs B, and Sandvig K (1999) Extraction of cholesterol with methyl-β-cyclodextrin perturbs formation of clathrin-coated endocytic vesicles. *Mol Biol Cell* **10:**961–974.
Ross EM and Wilkie TM (2000) GTPase-activating proteins for heterotrimeric G proteins: regulators of G protein signaling (RGS) and RGS-like proteins. *Annu Rev Biochem* **69:**795–827.
Shaul PW and Anderson RG (1998) Role of plasmalemmal caveolae in signal transduction. *Am J Physiol* **275:**L843–L851.
Shogomori H and Futerman AH (2001) Cholera toxin is found in detergent-insoluble rafts/domains at the cell surface of hippocampal neurons but is internalized via a raft-independent mechanism. *J Biol Chem* **276:**9182–9188.
Simons K and Toomre D (2000) Lipid rafts and signal transduction. *Nat Rev Mol Cell Biol* **1:**31–41.
Steinberg SF and Brunton LL (2001) Compartmentation of G protein-coupled signaling pathways in cardiac myocytes. *Annu Rev Pharmacol Toxicol* **41:**751–773.
Subtil A, Gaidarov I, Kobylarz K, Lampson MA, Keen JH, and McGraw TE (1999) Acute cholesterol depletion inhibits clathrin-coated pit budding. *Proc Natl Acad Sci USA* **96:**6775–6780.
Tsao PI and von Zastrow M (2000) Type-specific sorting of G protein-coupled receptors after endocytosis. *J Biol Chem* **275:**1130–1140.
Tsao PI and von Zastrow M (2001) Diversity and specificity in the regulated endocytic membrane trafficking of G-protein-coupled receptors. *Pharmacol Ther* **89:**139–147.
Wedegaertner PB (1998) Lipid modifications and membrane targeting of G alpha. *Biol Signals Recept* **7:**125–135.
Wedegaertner PB, Bourne HR, and von Zastrow M (1996) Activation-induced subcellular redistribution of Gs alpha. *Mol Biol Cell* **7:**1225–1233.
Weiss TS, Chamberlain CE, Takeda T, Lin P, Hahn KM, and Farquhar MG (2001) Gαi3 binding to calnuc on Golgi membranes in living cells monitored by fluorescence resonance energy transfer of green fluorescent protein fusion proteins. *Proc Natl Acad Sci USA* **98:**14961–14966.
Whistler JL, Tsao PI, and von Zastrow M (2001) A Phosphorylation-regulated brake mechanism controls the initial endocytosis of opioid receptors but is not required for post-endocytic sorting to lysosomes. *J Biol Chem* **276:**34331–34388.
Yu JZ and Rasenick MM (2002) Real-time visualization of a fluorescent $G_{\alpha s}$: dissociation of the activated G protein from plasma membrane. *Mol Pharmacol* **61:**352–359.

Address correspondence to: Dr. Marilyn G. Farquhar, Department of Cellular and Molecular Medicine, University of California, San Diego, 9500 Gilman Drive, La Jolla, CA, 92093-0651. E-mail: mfarquhar@ucsd.edu